

Polypyrrole Based Nanotheranostic Agent for MRI Guided Photothermal-Chemodynamic Synergistic Cancer Therapy

Bangyi Zhou¹, Chenhui Yin¹, Qiang Feng¹, Yiting Wu¹, Xiaoyu Pan¹, Chuang Liu²,

Jinjin Tian¹, Siqi Geng³, Kexin Wang¹, Jie Xing², Yi Cao², Pingbo Shou¹,

Zhangsen Yu^{*1}, Aiguo Wu^{*2}

¹ Laboratory of Nanomedicine, Medical Science Research Center, School of Medicine, Shaoxing University, Shaoxing City, Zhejiang Province, 312000, P. R. China

² Cixi Institute of Biomedical Engineering, CAS Key Laboratory of Magnetic Materials and Devices, Zhejiang Engineering Research Center for Biomedical Materials, Ningbo Institute of Materials Technology and Engineering, Chinese Academy of Sciences, Ningbo, Zhejiang Province, 315201, P. R. China

³ College of Life Science, Shaoxing University, Shaoxing City, Zhejiang Province, 312000, P. R. China

** Corresponding author: yzs@usx.edu.cn, aiguo@nimte.ac.cn*

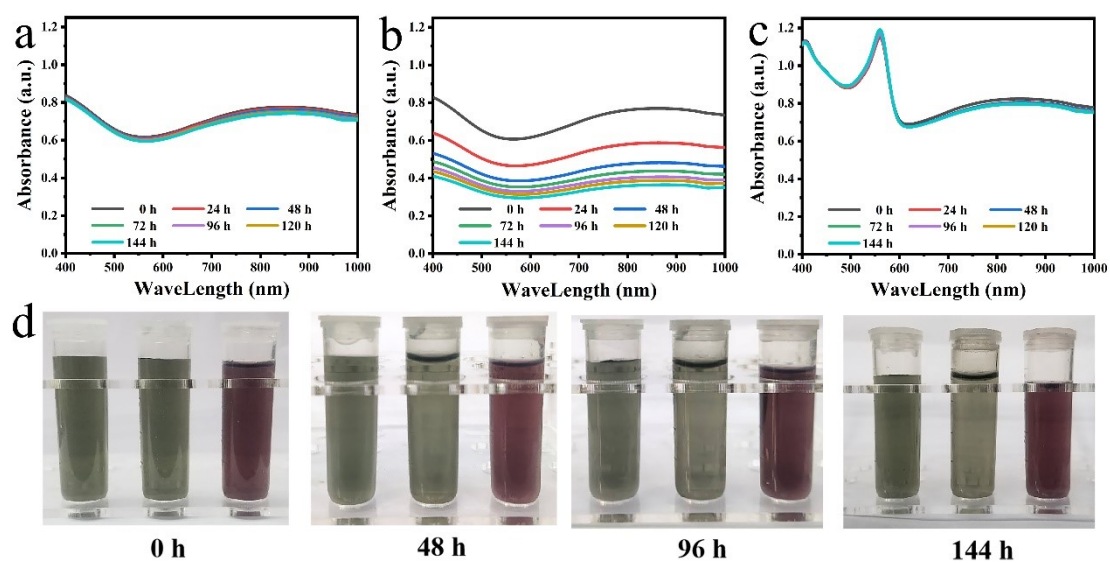


Fig. S1. (a-c) The Vis-NIR spectra of PBM(5) nanoprobes in deionized water, phosphate-buffered saline, and cell culture medium; (d) Photographs of the PBM(5) nanoprobes dispersed in different solvents that from left to right are deionized water, phosphate-buffered saline, and culture medium.

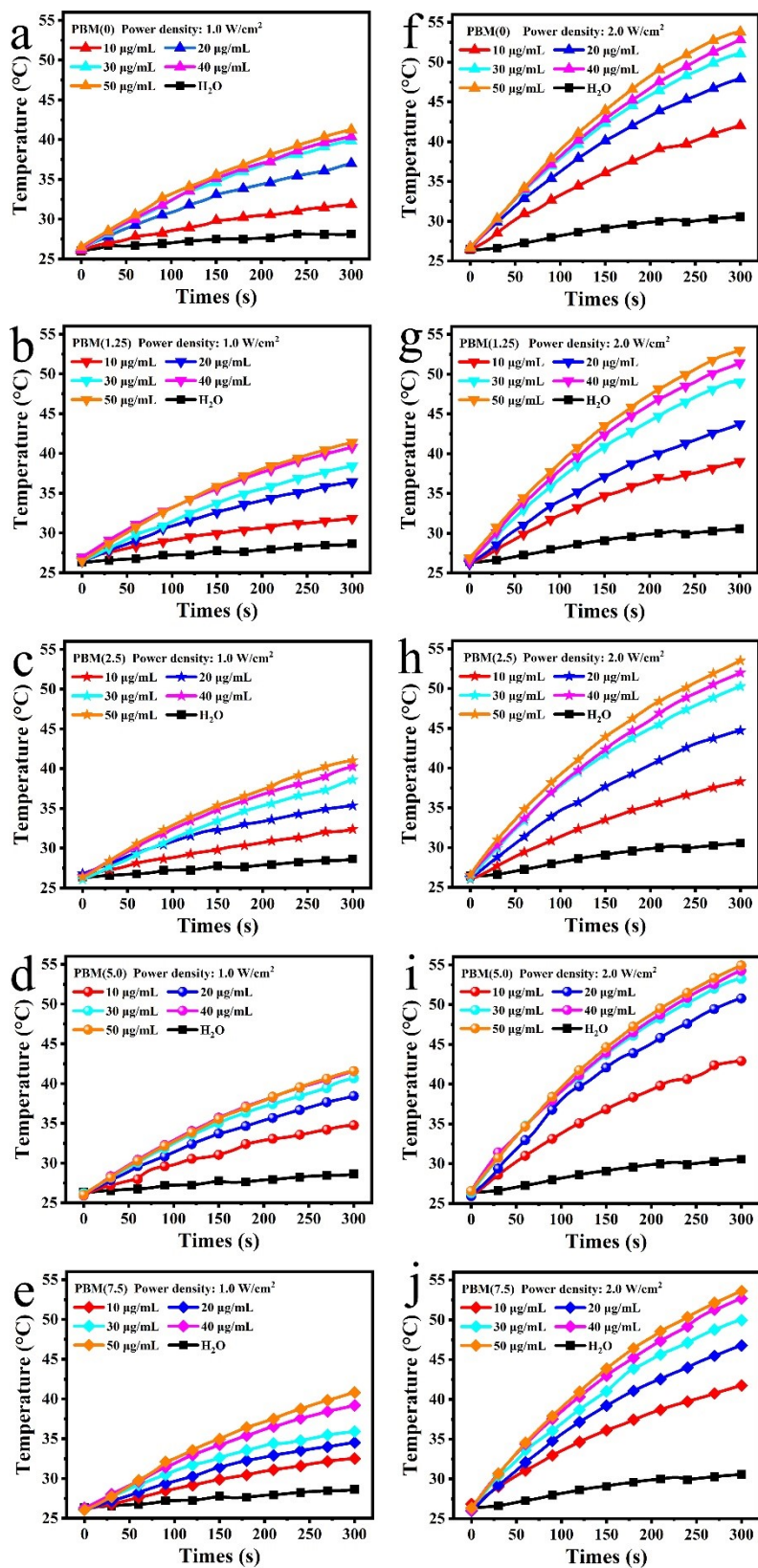


Figure S2. The temperature rise curves of different PBM(n) nanoprobcs under irradiation with an 808 nm laser of 1.0 (a, b, c, d, e) and 2.0 (f, g, h, i, j) W cm^{-2} for 5 min.

Samples	τ_s (s)	hs (W °C ⁻¹)	$\Delta T = T_{\max} - T_{\text{surr}}$ (°C)	Q_{dis} (W)	I (W cm ⁻²)	$A_{808 \text{ nm}}$	η
PBM(0)	439.9	0.00764	40.89	0.0444	1.0	0.996	29.80%
PBM(1.25)	457.6	0.00734	40.02			1.007	27.66%
PBM(2.5)	452.2	0.00743	40.09			1.024	27.99%
PBM(5.0)	465.3	0.00722	40.1			1.007	27.19%
PBM(7.5)	425.3	0.00790	40.02			1.038	29.93%

Table S1. The specific values of the τ_s , hs , ΔT , Q_{dis} , laser power density, and absorbance at 808 nm are used for calculating the photothermal conversion efficiency of the PBM(n) nanoprobcs.

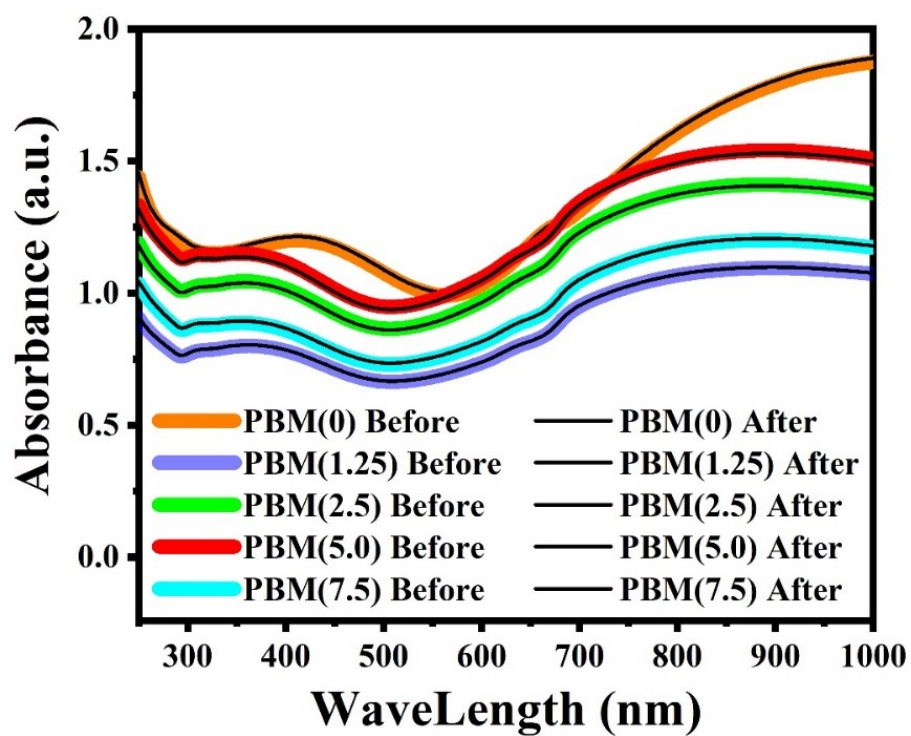


Fig. S3. Absorbance spectra of PBM(n) nanoprobe before and after 5 min of 808 nm laser irradiation (2.0 W cm^{-1}).

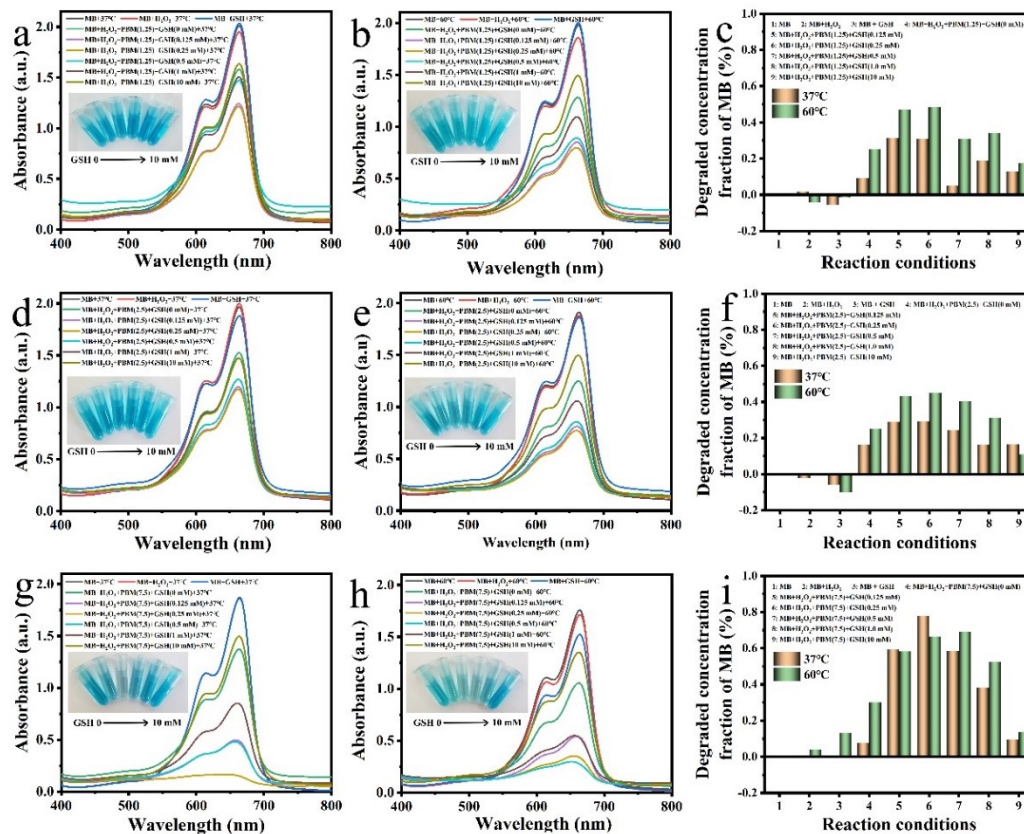


Fig. S4. The *in vitro* Fenton-like reaction of methylene blue degradation by PBM(1.25) (a-c), PBM(2.5) (d-f), and PBM(7.5) (g-i). The UV-Visible absorption spectra, pictures, and degradation rates of methylene blue before and after degradation by PBM(n) mediated Fenton-like reaction under different experimental conditions. Each nanoprobe was evaluated at 37 °C and 60 °C, respectively.

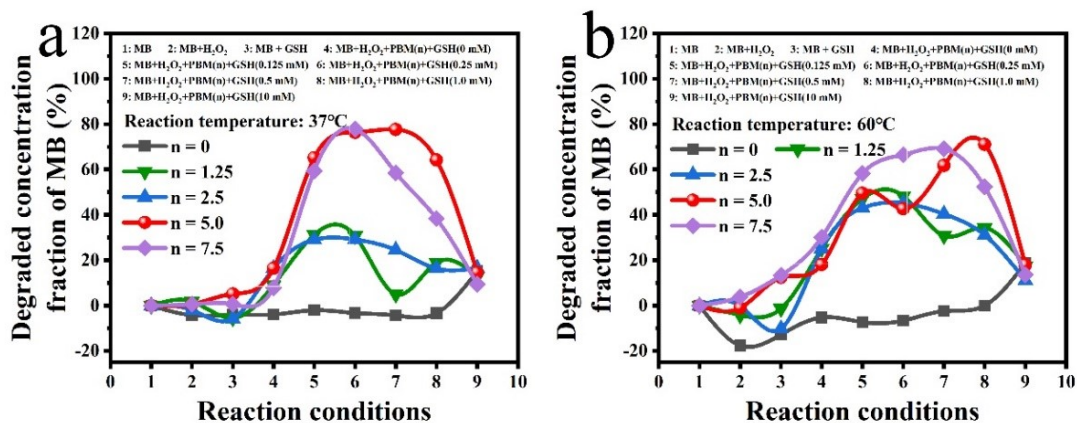


Fig. S5. The degradation rate curves of PBM(n) nanoprobe degraded methylene blue through Fenton-like reaction under 37°C (a) and 60°C (b) with different experimental conditions.

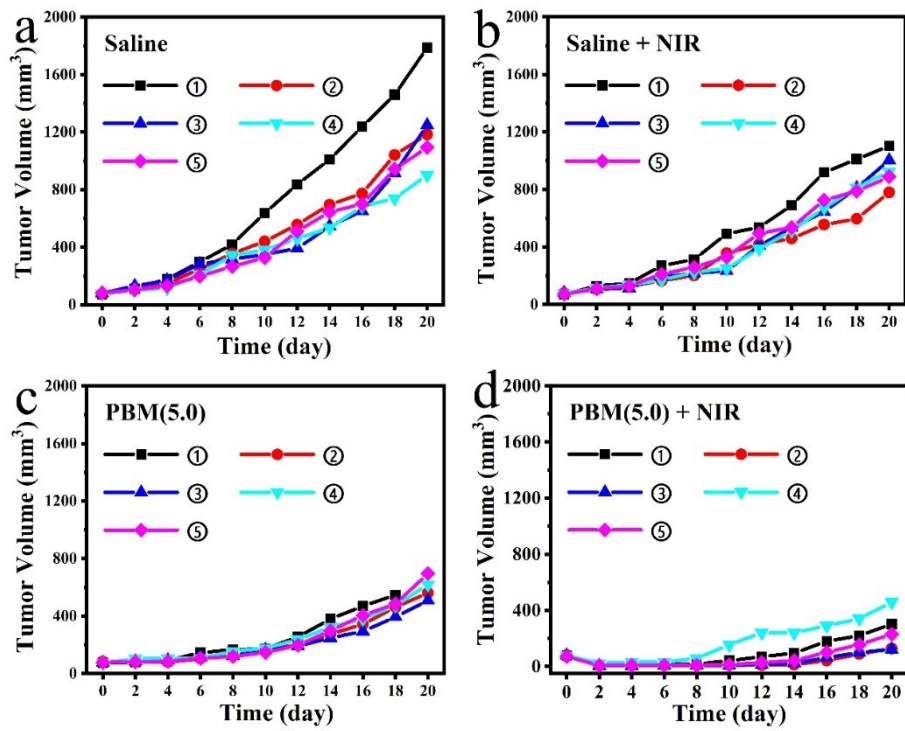


Fig. S6. Tumor growth curves of 808 nm laser irradiated and unirradiated tumors in individual mice treated with saline or PBM(5.0) nanoprobes. (a) Saline, (b) Saline + NIR, (c) PBM(5.0), (d) PBM(5.0) + NIR.

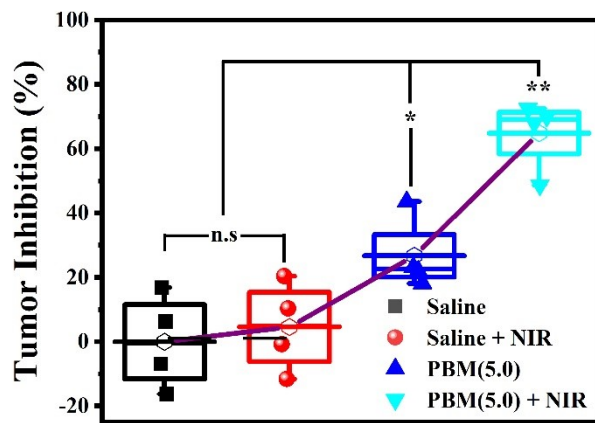


Fig. S7 Tumor inhibitions (%) of mice on the 20th day after different treat groups.

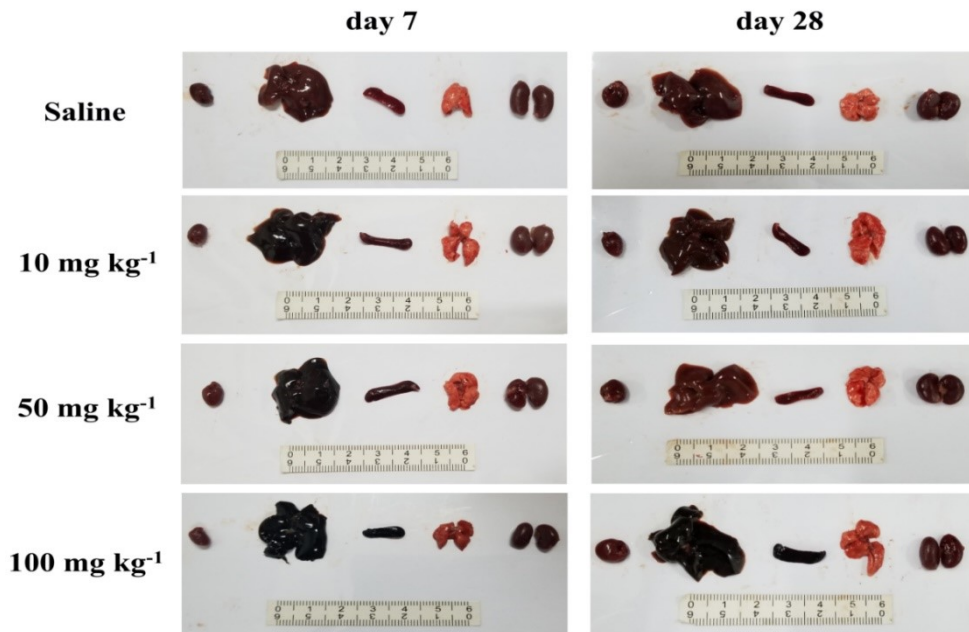


Fig. S8. Main organs photograph of mice treated with different concentrations of PBM(5) nanoprobe. Three mice in each group were sacrificed on day 7 and the rest on day 28. From left to right are the heart, liver, spleen, lung, and kidney.

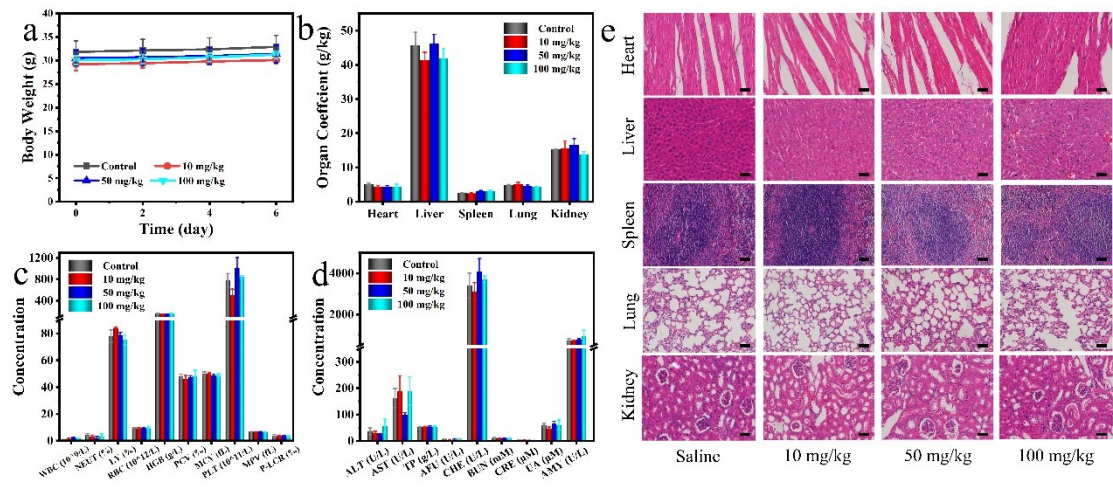


Fig. S9. *In vivo* assessment acute toxicity of tail intravenous administration different doses PBM(5.0) nanoprobe for healthy male ICR mice for 7 days. (a-d) Body weights, vital organs coefficient, main indicators of blood routine, and serum biochemistry of mice after various treatments; (e) Histological analyses of tissue slices (heart, liver, spleen, lung, and kidney) collected from different groups of mice after various treatments. Scale bars: 100 μ m.